02 Apr 2024

Chiral Recognition of Chiral (Hetero)Cyclic Derivatives Probed by Tetraaza Macrocyclic Chiral Solvating Agents Via ^{1}H NMR Spectroscopy

Yu Wang

Hongmei Zhao

Chunxia Yang

Lixia Fang

et. al. For a complete list of authors, see https://scholarsmine.mst.edu/chem_facwork/3690

Recommended Citation

Y. Wang et al., "Chiral Recognition of Chiral (Hetero)Cyclic Derivatives Probed by Tetraaza Macrocyclic Chiral Solvating Agents Via ^{1}H NMR Spectroscopy," *Analytical Chemistry*, vol. 96, no. 13, pp. 5188 - 5194, American Chemical Society, Apr 2024.
The definitive version is available at https://doi.org/10.1021/acs.analchem.3c05395

analytical chemistry

pubs.acs.org/ac Article

Chiral Recognition of Chiral (Hetero)Cyclic Derivatives Probed by Tetraaza Macrocyclic Chiral Solvating Agents via ^{1}H NMR Spectroscopy

Yu Wang, Hongmei Zhao, Chunxia Yang, Lixia Fang, Li Zheng, Hehua Lv, Pericles Stavropoulos, Lin Ai,* and Jiaxin Zhang*

Cite This: *Anal. Chem.* 2024, 96, 5188−5194 Read Online

ACCESS | Metrics & More | Article Recommendations | Supporting Information

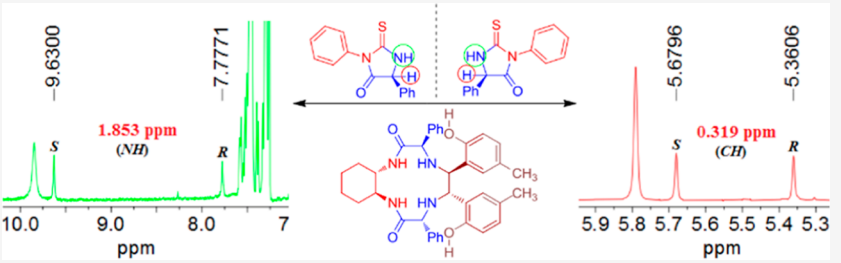

ABSTRACT: In the field of chiral recognition, chiral cyclic organic compounds, especially heterocyclic organic compounds, have attracted little attention and have been rarely studied as chiral substrates by means of ^{1}H NMR spectroscopy. In this paper, enantiomers of thiohydantoin derivatives, representing typical five-membered *N*,*N*-heterocycles, have been synthesized and utilized for assignment of absolute configuration and analysis of enantiomeric excess. All enantiomers have been successfully differentiated with the assistance of novel tetraaza macrocyclic chiral solvating agents (TAMCSAs) by ^{1}H NMR spectroscopy. Surprisingly, unprecedented nonequivalent chemical shift values (up to 2.052 ppm) of the NH proton of substrates have been observed, a new milestone in the evaluation of enantiomers. To better understand the intermolecular interactions between host and guest, Job plots and theoretical calculations of (*S*)-G**1** and (*R*)-G**1** with TAMCSA **1a** were investigated and revealed significant geometric differentiation between the diastereomers. In order to evaluate practical applications of the present systems in analyzing optical purity of chiral substrates, enantiomeric excesses of a typical substrate (G**1**) with different optical compositions in the presence of a representative TAMCSA (**1a**) can be accurately calculated based on the integration of the NH proton's signal peaks. Importantly, this work provides a significant breakthrough in exploring and developing the chiral recognition of chiral heterocyclic organic compounds by ^{1}H NMR spectroscopy.

Nuclear magnetic resonance (NMR) spectroscopy plays an increasingly important role as a fast and powerful analytical tool in the field of chiral recognition, including the assignment of absolute configuration of chiral molecules and determination of enantiomeric excess of chiral compounds.[1−5] These parameters constitute important and fundamental characterization data in many related research areas, such as in the evaluation of asymmetric synthetic[6,7] and natural products,[8,9] as well as in fields such as food science[10−12] and chiral materials.[13,14] In particular, in chiral pharmaceutical chemistry, different enantiomers of chiral drugs have different biological and pharmaceutical activities, with one producing beneficial outcomes to combat human diseases, whereas the other one may have a detrimental, if not toxic effect to health.[15−17] Over the past decade, NMR spectroscopy, assisted by the use of chiral oriented solvents,[18,19] and especially chiral solvating agents (CSAs) as chiral auxiliaries, has received considerable attention in chiral recognition[20−23] due to several advantages, such as fast and convenient operation, accurate and reliable measurement, low sample consumption, and need for small amounts of deuterated solvent. In addition, multiple field windows are often available for observing split proton signals by ^{1}H NMR spectroscopy, an ubiquitous technique available in nearly all chemical and related laboratories.[24,25] However, developing highly sensitive, effective, and versatile chiral auxiliaries, especially CSAs, remains a challenging undertaking. In reported work, a few CSAs, such as chiral amines,[26] carboxylic acids,[27] amides,[28,29] crown ethers,[30,31] calixirenes,[32] and others,[33] have been developed and utilized for this purpose with the assistance of ^{1}H NMR spectroscopy. However, CSAs

Received: November 28, 2023
Revised: February 20, 2024
Accepted: March 4, 2024
Published: March 20, 2024

https://doi.org/10.1021/acs.analchem.3c05395
Anal. Chem. 2024, 96, 5188−5194

with outstanding features are still a scarce commodity. Herein, we report tetraaza macrocyclic chiral solvating agents (TAMCSAs) with unique structures containing two amide groups (CONHs), two phenolic hydroxyl groups (PhOHs), and two amino groups (NHs), along with an overall C_2-symmetry and a well-defined cavity, to further explore their chiral discriminating capability for a wide range of chiral substrates by means of ^{1}H NMR spectroscopy (Figure 1).

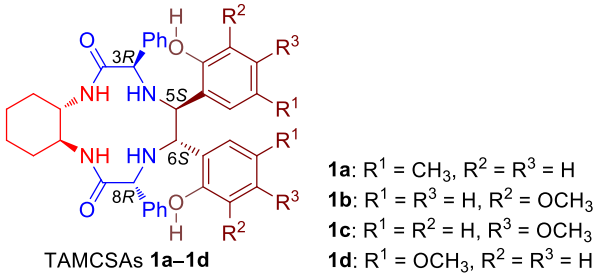

Figure 1. Structures of TAMCSAs **1a**−**1d**.

In our previous work, the potential chiral discriminating capability of a few TAMCSAs has been successfully evaluated by chiral recognition of α-hydroxy acids and *N*-Ts-α-amino acids with one chiral center,[34] dipeptide derivatives with two centers,[35] tripeptide derivatives with three centers,[36] and chiral ester derivatives.[37] These results show that TAMCSAs are highly sensitive, effective, and versatile CSAs.

In reported work, several chiral chain organic compounds have been often used as chiral substrates for the determination of the absolute configuration and evaluation of enantiomeric excess, including chiral amines,[38,39] alcohols,[39−41] amino alcohols,[39,42] carboxylic acids,[43,44] and amino acids or their derivatives.[45] On the other hand, chiral *cyclic* organic compounds have been scarcely investigated as chiral substrates by means of ^{1}H NMR spectroscopy.[46] Yet, single enantiomers of chiral cyclic organic compounds can have high biological and pharmaceutical activity and can be used as clinical chiral drugs, as well as in synthetic/catalytic applications. For example, the following thiohydantoin derivatives have been used as antiprostate cancer agents (Figure 2a)[47] and as chiral catalysts for iodoamination of alkenes (Figure 2b).[48]

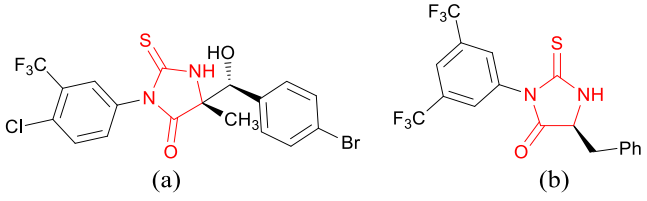

Figure 2. Structures of antiprostate cancer agent (a) and chiral alkene iodoamination catalyst (b).

In this paper, enantiomers of chiral thiohydantoin derivatives, as a representative class of five-membered *N*,*N*-heterocyclic organic compounds, were prepared and used as chiral substrates for chiral recognition in the presence of TAMCSAs by ^{1}H NMR spectroscopy.

EXPERIMENTAL SECTION

Synthesis of TAMCSAs 1a−1d. Chiral diimines **3a**−**3d** (Figure 3a) were prepared from 1,2-(1*S*,2*S*)-(+)-cyclohexanediamine and D-phenylglycine in three steps and 80−85% yields and were used without further purification, according to a literature protocol.[49] TAMCSAs **1a**−**1d** were synthesized by the intramolecular reductive C−C coupling reaction of **3a**−**3d** at −18−0 °C in a dried DMF dilute suspension under the nitrogen atmosphere[50,51] and were further purified by column chromatography on silica gel to afford enantiopure compounds in 13−25% yields. Meanwhile, chiral compounds **2a**−**2d** (Figure 3b) were obtained as byproducts in 11−15% yields. The detailed synthetic routes and procedures are available in the Supporting Information (page S-3).

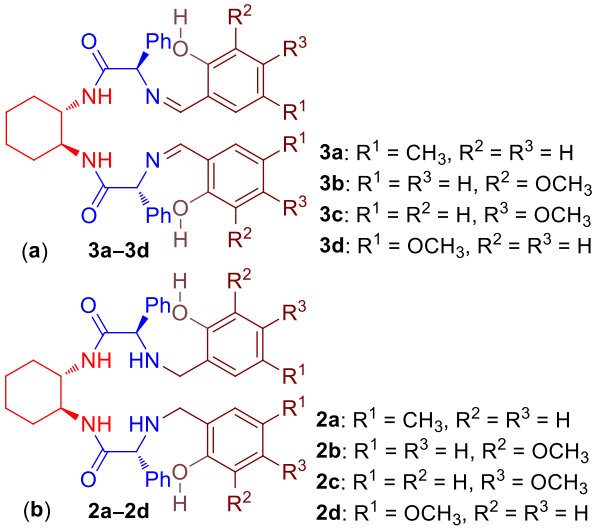

Figure 3. Structures of chiral compounds **2a**−**2d** and **3a**−**3d**.

TAMCSAs **1a**−**1c** and chiral compounds **2a**−**2c** were characterized as new compounds by ^{1}H NMR, ^{13}C NMR, HRMS, and IR methods with the exception of TAMCSA **1d** and **2d**, which have been previously reported.[34] Crystals of TAMCSA **1c** suitable for single-crystal X-ray diffraction were obtained through slow evaporation of acetone solution at ambient temperature. Absolute configurations of the newly generated chiral carbon atoms (C15 and C23) of the ArCH*NH groups of TAMCSA **1c** were assigned to possess *S*, *S* chirality based on X-ray crystallographic analysis (Figure 4).

Unfortunately, crystals of TAMCSAs **1a** and **1b** suitable for X-ray diffraction analysis were not obtained. Therefore, their NOESY spectra were examined for assignment of the absolute configuration of the two newly produced chiral carbon atoms of the ArCH*NH groups. The hydrogen atoms (ArCH*NH) of TAMCSAs **1a** and **1b** show strong NOESY correlated ^{1}H NMR signals with the two CH protons (α-H) of the D-phenylglycine moieties. This result suggests that two pairs of closely spaced hydrogen atoms of TAMCSAs **1a** and **1b** (α-*H*s and ArCH*NHs, 3*R* and 5*S*, and 8*R* and 6*S*) are located on the same side of the macrocyclic framework (Figure 1). Based on these NOESY spectra, the absolute configurations of the newly generated chiral carbon atoms (ArCH*NH) of TAMCSAs **1a** and **1b** have been assigned as *S*, *S*. The structural characterization data and spectra are available in the Supporting Information (pages S-3−S-4 and S-21−S-30).

Synthesis of Enantiomers of Thiohydantion Derivatives G1−G13. Enantiomers of thiohydantoin derivatives G1−G7 (R^1 = H) were prepared from D- and L-α-amino acids with phenyl isothiocyanate according to the reported synthetic

https://doi.org/10.1021/acs.analchem.3c05395
Anal. Chem. 2024, 96, 5188−5194

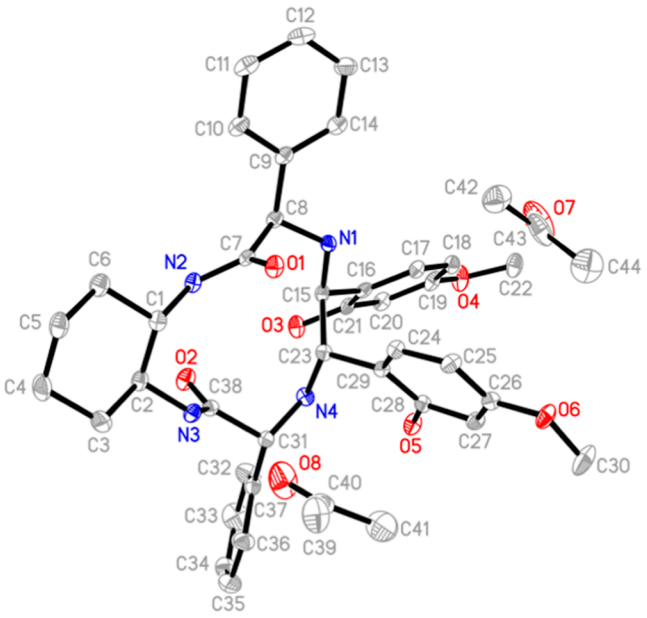

Figure 4. X-ray crystal structure of TAMCSA **1c**·2·$(CH_3)_2CO$ drawn at 30% probability thermal ellipsoids.

procedure in 50−80% yields.[52] In order to compare the electronic effects of different substituent groups of the chiral thiohydantoin derivatives on chiral discrimination, the enantiomers of G**8**−G**13** (R^1 = CF_3) were prepared from 3,5-*bis*(trifluoromethyl)phenyl isothiocyanate with D- and L-*α*-amino acids, containing the same amino acid moieties (Figure 5).

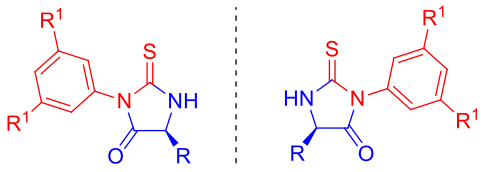

R^1 = H,
G**1**: R = Ph
G**2**: R = $PhCH_2$
G**3**: R = CH_3
G**4**: R = $CH(CH_3)_2$
G**5**: R = $CH_2CH(CH_3)_2$
G**6**: R = $(CH_2)_2SCH_3$
G**7**: R = CH_2OH

R^1 = CF_3,
G**8**: R = Ph
G**9**: R = $PhCH_2$
G**10**: R = CH_3
G**11**: R = $CH(CH_3)_2$
G**12**: R = $CH_2CH(CH_3)_2$
G**13**: R = $(CH_2)_2SCH_3$

Figure 5. Structures of the enantiomers of thiohydantoin derivatives.

Among them, the chemical structures of (*S*)-G**8**, (*S*)-G**12**, and (*R*)-G**8**−**13** constitute new optically pure compounds and have been characterized by ^{1}H NMR, ^{13}C NMR, ^{19}F NMR, HRMS, and IR methods. Detailed synthetic routes and procedures are available in the Supporting Information (pages S-5−S-7 and S-31−S-46).

Chiral Recognition of Enantiomers of Thiohydantion Derivatives G1−G13. ^{1}H NMR spectra of (±)-G**1**−G**13** were measured in the presence of TAMCSAs **1a**−**1d** in $CDCl_3$ on a 400 MHz spectrometer based on the optimized chiral discriminating conditions (molar ratio of host and guest = 1:1 and a concentration of 5 mM in most cases).

RESULTS AND DISCUSSION

To explore the discrimination of enantiomers of chiral thiohydantoin derivatives and evaluate the chiral discriminating capability of TAMCSAs **1a**−**1d**, a sample of (±)-G**1** with TAMCSA **1a** (molar ratio = 1:1) was prepared at a concentration of 5 mM in $CDCl_3$, and its ^{1}H NMR spectrum was measured on a 400 MHz spectrometer. The results show that an unprecedented nonequivalent chemical shift value ($\Delta\Delta\delta$ = 1.853 ppm) was observed by means of separated ^{1}H NMR signals of the NH proton of (±)-G**1**, with a high baseline resolution. Meanwhile, $\Delta\Delta\delta$ (0.319 ppm) of the CH proton was also exhibited. Subsequently, a sample of (*S*)-G**1** was added to the aforementioned solution of (±)-G**1** with TAMCSA **1a**, and its ^{1}H NMR spectrum was measured under the same conditions. The absolute configuration of enantiomers of (±)-G**1** were easily determined by the change of the integration of ^{1}H NMR signal peak areas of the split protons. Partial expanded spectra and $\Delta\Delta\delta$ values of the split protons (NH and CH) of (±)-G**1** in the presence of TAMCSA **1a** are shown in Figure 6.

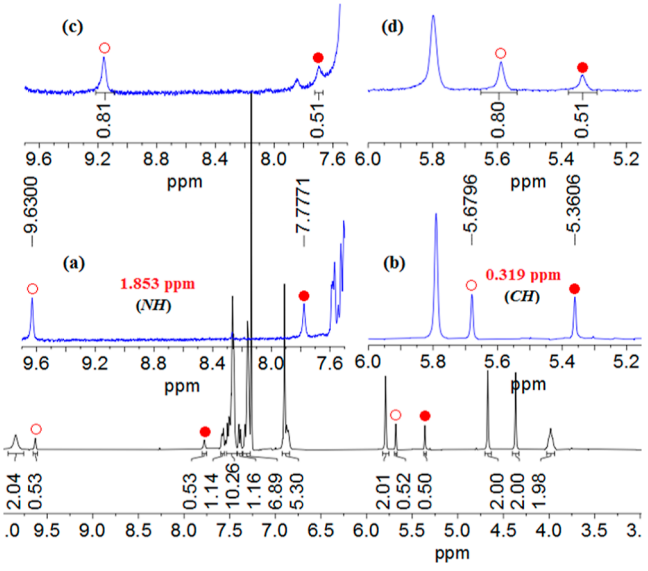

Figure 6. ^{1}H NMR spectrum and expanded spectra of (±)-**G1** (a,b), and (*S*)-G**1**/(*R*)-G**1** (1.6:1) (c,d) in the presence of TAMCSA **1a** in $CDCl_3$ (400 MHz), [TAMCSA **1a**] = 5 mM, "○ (red)" stand for (*S*)-G**1**, "● (red)" stands for (*R*)-G**1**.

Encouraged by these remarkable chiral discriminating results, we sought to obtain better chiral discriminating effects, including superior baseline resolution and more clearly separated ^{1}H NMR signals with fewer (if any) overlapping peaks. To this effect, chiral discriminating conditions were screened and optimized by ^{1}H NMR measurements involving different concentrations and molar ratios of host and guest. Based on these results, a concentration of 5 mM of guest (in most cases) and 1:1 molar ratio of host and guest are more suitable for this study. Their partial ^{1}H NMR spectra are available in the Supporting Information (page S-7, Figures S2 and S3).

Under optimized chiral discriminating conditions, 51 samples of (±)-G**1**−**13** were prepared in the presence of TAMCSAs **1a**−**1d** in $CDCl_3$, and their ^{1}H NMR spectra were measured on a 400 MHz spectrometer, with the exception of the (±)-G**1** and TAMCSA **1a** combination, which has been

https://doi.org/10.1021/acs.analchem.3c05395
Anal. Chem. 2024, 96, 5188−5194

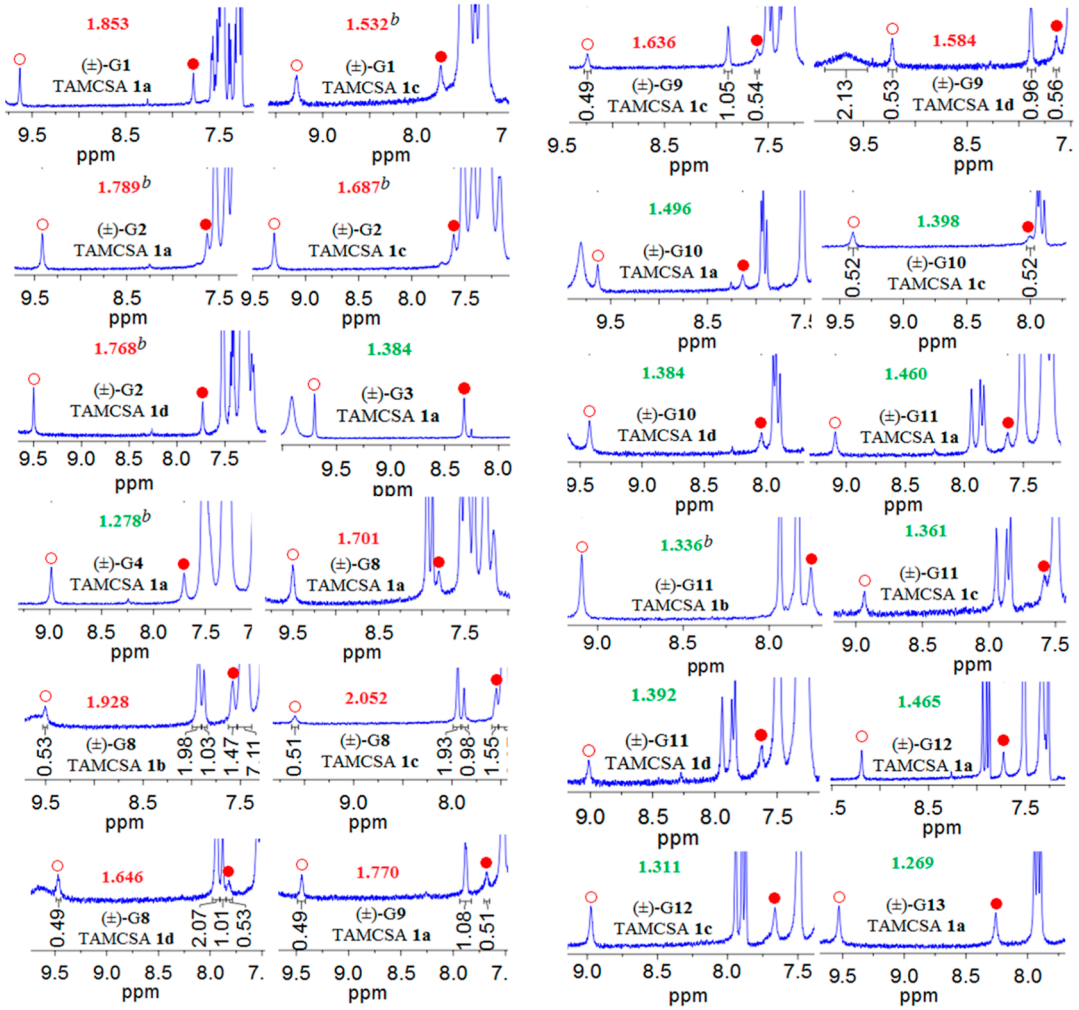

Figure 7. Nonequivalent chemical shift values ($\Delta\Delta\delta \geq 1.269$ ppm) and partial spectra of the NH proton of (±)-G**1**−G**4**, and (±)-G**8**−G**13** in the presence of TAMCSAs **1a**−**1d** in $CDCl_3$ (400 MHz) at a concentration of 5 mM, and [b]10 mM; [○ (red)] and [● (red)] stand for (*S*)- and (*R*)-enantiomers; $\Delta\Delta\delta = |\Delta\delta_S - \Delta\delta_R|$, $\Delta\delta_S = \delta_S - \delta_{free}$, $\Delta\delta_R = \delta_R - \delta_{free}$. ^{1}H NMR spectra of all examples in this work were measured on a JEOL spectrometer at 400 MHz (type of NMR probe: broadband gradient autotune).

measured under the aforementioned optimized conditions [1:1 molar ratio of (±)-G**1** and TAMCSA **1a**, [(±)-G**1**] = 5 mM]. The results show that the enantiomers of all thiohydantoin derivatives were clearly differentiated by the separated ^{1}H NMR signals of the related protons of (±)-G**1**−**13** in the presence of TAMCSAs **1a**−**1d**. Different chemical shifts for multiple types of protons of enantiomers of all of the thiohydantoin derivatives were clearly exhibited. Importantly, several highly significant chiral discriminating outcomes were obtained in the ^{1}H NMR spectra of (±)-G**1**−**13**. Among 52 samples, $\Delta\Delta\delta$ values (red) of the NH proton of 12 samples exceed 1.530 ppm. Most astonishingly, the maximum $\Delta\Delta\delta$ value of the NH proton of (±)-G**8** is as high as 2.052 ppm in the presence of TAMCSA **1c**. In addition, $\Delta\Delta\delta$ values (green) of the NH proton of 33 samples are between 1.024 and 1.496 ppm. The $\Delta\Delta\delta$ values (blue) of the NH proton of seven samples range between 0.582 and 0.942 ppm. To the best of our knowledge, such large nonequivalent chemical shift values (up to 2.052 ppm) have never been previously observed in the presence of CSAs by means of ^{1}H NMR spectroscopy. Subsequently, samples of (*S*) or (*R*)-G**1**−**13** were added to the aforementioned solution of (±)-G**1**−**13** with TAMCSAs **1a**−**1d**, and their ^{1}H NMR spectra were also measured on a 400 MHz spectrometer under the same conditions. The assignments of enantiomers of (±)-G**1**−**13** were easily determined based on integration changes of the ^{1}H NMR signal peak areas of the corresponding split protons. The $\Delta\Delta\delta$ values and partial spectra of the NH proton, as the most representative case ($\Delta\Delta\delta \geq 1.269$ ppm, 24 samples), are summarized in Figure 7. $\Delta\Delta\delta$ values and partial spectra of other NH protons ($\Delta\Delta\delta <$ 1.269 ppm, 28 samples), with the exception of $\Delta\Delta\delta$ values of other split protons of chiral thiohydantoin derivatives, are available in the Supporting Information (pages S-8−S-10, Figure 5S, Table S2).

Moreover, remarkable changes of chemical shifts ($\Delta\delta$, ppm) of the *NH* proton of enantiomers of (±)-G**1**−**13** were also observed in the presence of TAMCSAs **1a**−**1d**. Compared with chemical shift values of the NH proton of free (±)-G**1**−**13**, chemical shifts of the NH proton of the (*S*)-enantiomer of the aforementioned guests shifted drastically downfield (by up to 2.025 ppm, $\Delta\delta_S = \delta_S - \delta_{free}$). However, chemical shifts of the NH proton of the (*R*)-enantiomer moved slightly downfield or upfield ($\Delta\delta_R = \delta_R - \delta_{free}$) in most cases. These results suggest that the diastereomeric complexes of (±)-G**1**−**13** with TAMCSAs **1a**−**1d** exhibit larger geometric variances, presumably due to differential intermolecular interactions

https://doi.org/10.1021/acs.analchem.3c05395
Anal. Chem. 2024, 96, 5188−5194

between hosts and the two enantiomers of guests. Detailed changes of chemical shift values of the NH proton of (±)-G**1**−**13** in the presence of TAMCSAs **1a**−**1d** are available in the Supporting Information (page S-10, Table S3).

In addition, in order to investigate the temperature effect on enantiodifferentiation, a sample of (±)-G**6** with TAMCSA **1a** in $CDCl_3$ was prepared (molar ratio = 1:1, 5 mM), and its ^1H NMR spectra were measured on a 400 MHz spectrometer from 298 to 248 K. The results show that $\Delta\Delta\delta$ of the NH proton of (±)-G**6** becomes larger, ranging from 1.074 ppm (298 K) to 1.211 ppm (258 and 253 K) as the temperature gradually decreases. However, at 248 K, the $\Delta\Delta\delta$ value (1.208 ppm) of the NH proton of (±)-G**6** starts to get smaller than that (1.211 ppm) at 253 and 258 K, because samples started precipitating, as the temperature decreased (Figure 8).

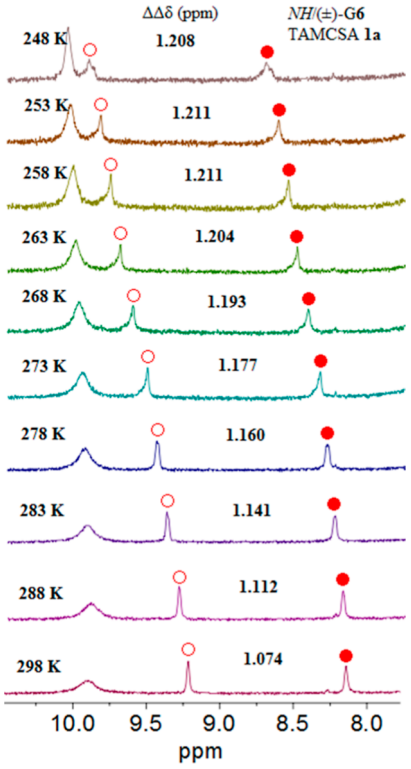

Figure 8. Nonequivalent chemical shift values ($\Delta\Delta\delta$, ppm) and partial spectra of the NH proton of (±)-G**6** in the presence of TAMCSA **1a** at different temperatures in $CDCl_3$ (400 MHz). [○ (red)] and [● (red)] stand for (*S*)- and (*R*)-G**6**.

Encouraged by the unprecedented nonequivalent chemical shift values noted above, we were keenly interested in investigating the type of intermolecular interactions between host and guest and deducing a possible mechanism of chiral recognition. First, Job plots of (±)-G**1** were obtained in the presence of TAMCSA **1a** by ^1H NMR titration experiments.[53] A maximum value ($X \times \Delta\delta_{SR}$ = 0.121 ppm, $X \times \Delta\delta_S$ = 0.141 ppm, $X \times \Delta\delta_R$ = 0.020 ppm) of the NH proton of (±)-G**1** was exhibited at a molar fraction of X = 0.5 in the presence of TAMCSA **1a** (Figure 9).

This result suggests that a pair of diastereomeric complexes with 1:1 stoichiometry is formed between (±)-G**1** and TAMCSA **1a**.

To further understand the intermolecular interaction between (±)-**G1** and TAMCSA **1a**, the geometries of (*R*)-G**1** and (*S*)-G**1** with TAMCSA **1a** were optimized by using density functional theory (DFT) at the B3LYP/3-21G* level.[54] The continuum model (SMD) for chloroform was used in all NMR calculations to simulate the solvent effects. The proposed models show that two hydrogen bonds are formed between (*R*)-G**1** and TAMCSA **1a** (NH···(H)OPh, 2.062 Å; PhNCO···HNCO, 1.902 Å) (Figure 10a). However, only one strong hydrogen bond is formed between (*S*)-G**1** and TAMCSA **1a** (NH···OCNH) with a bond length of 1.779 Å (Figure 10b).

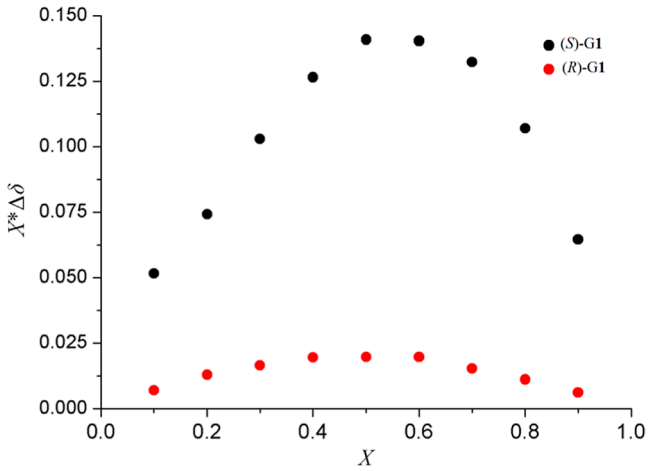

Figure 9. Job plots for complexes of (*S*)-G**1** and (*R*)-G**1** with TAMCSA **1a**. $\Delta\delta$ stands for chemical shift change of the NH proton of (*R*)-G**1** [(●) red] and (*S*)-G**1** (●) in the presence of TAMCSA **1a** in $CDCl_3$ at room temperature (400 MHz). *X* stands for the molar fraction of (±)-G**1**, (X = [(±)-G**1**]/[(±)-G**1** + TAMCSA **1a**]).

The chemical shift values (δ, ppm) of the NH proton of (*R*)-G**1** and (*S*)-G**1** in the presence of TAMCSA **1a** and their equivalent chemical shift ($\Delta\delta$, ppm) are obtained by DFT/SMD calculations. These results are in agreement with the observed chemical shift values and nonequivalent chemical shift values of the same proton (as shown in the Supporting Information, page S-11, Table S4). The Cartesian coordinates and total energies of the complexes of (*S*)-G**1** and (*R*)-G**1** with TAMCSA **1a** are obtained by means of B3LYP/3-21G* structural optimization and are available in the Supporting Information (pages S-11−S-21, Tables S5−S9).

Now that the chiral discriminating capability of TAMCSAs **1a**−**1d** has been effectively established by examining the differentiation of chiral thiohydantoin derivatives (±)-G**1**−**13**, and practical application in determining enantiomeric purity can be further explored. Subsequently, samples containing (*S*)-G**6** with 10, 20, 30, 50, 70, 85, and 90% ee were prepared in the presence of TAMCSA **1a** in $CDCl_3$ at room temperature, and their ^1H NMR spectra were measured on a 400 MHz NMR spectrometer. Enantiomeric excesses (ee) for all samples were accurately calculated based on the integration of the NH proton of (*S*)-G**6** and (*R*)-G**6**, featuring well-separated ^1H NMR signals, and with large enough nonequivalent chemical shifts and good baseline resolution (Figure 11). Excellent linear correlation between the theoretical (X) and observed (Y) ee % values was obtained in the presence of TAMCSA **1a** (as shown in Supporting Information page S-8, Figure S4).

CONCLUSIONS

In summary, chiral recognition by means of ^1H NMR spectroscopy has been successfully investigated by virtue of

https://doi.org/10.1021/acs.analchem.3c05395
Anal. Chem. 2024, 96, 5188−5194

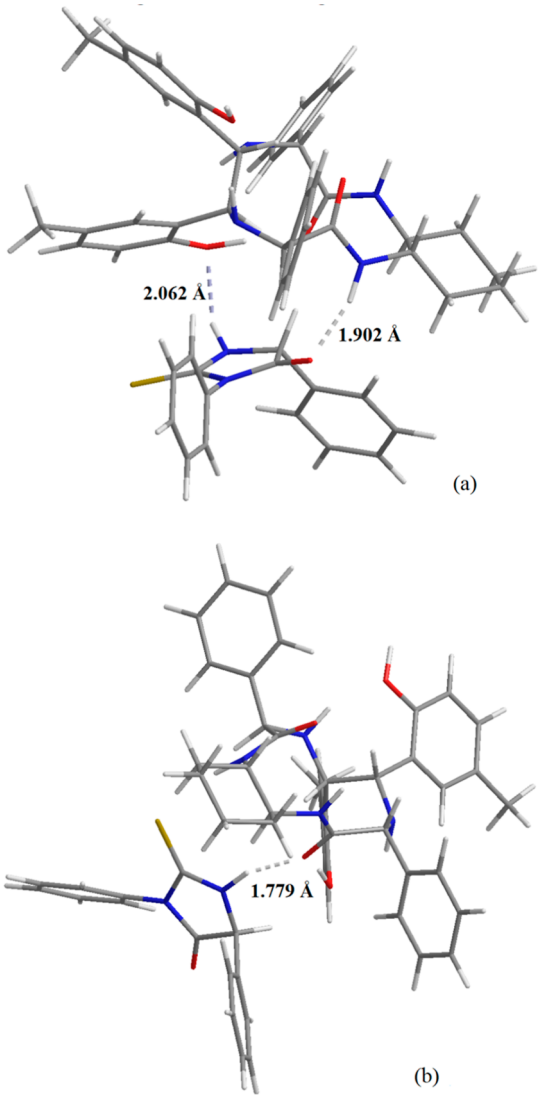

Figure 10. Proposed DFT models for the hydrogen bonding interactions between TAMCSA **1a** and (*R*)-G**1** (a) and (*S*)-G**1** (b).

outstanding differentiations of chemical shifts of the split protons of enantiomers of thiohydantoin derivatives (±)-G**1**−**13**. Surprisingly large nonequivalent chemical shift values (up to 2.052 ppm) of enantiomers of thiohydantoin derivatives in the presence of TAMCSAs **1a**−**1d** have been established. Practical applications in the analysis of enantiomeric excess (ee) have been achieved by evaluating the integration area of the NH proton of G**1** (up to 90% ee) with the assistance of TAMCSA **1a**. In addition, the intermolecular interaction between G**1** and TAMCSA **1a** has been explored by Job plots and theoretical chemical calculations. More importantly, this work provides a new benchmark in the field of chiral recognition by ^{1}H NMR spectroscopy since unprecedented nonequivalent chemical shifts of chiral thiohydantoin derivatives have been observed in the presence of a family of highly sensitive and effective TAMCSAs. Furthermore, this work also provides a significant breakthrough in exploring and developing the chiral recognition of chiral heterocyclic compounds, especially chiral *N*,*N*-heterocyclic organic compounds as potential chiral drugs, by means of ^{1}H NMR spectroscopy.

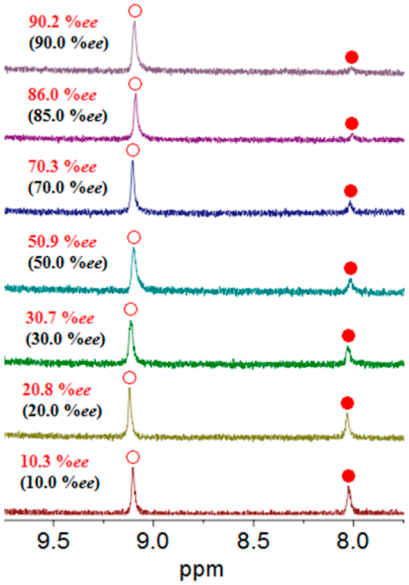

Figure 11. Determination of enantiomeric excesses of G**6** with different optical purities, *ee* (%) = {[(*S*)-G**6** − (*R*)-G**6**]/[(*S*)-G**6** + (*R*)-G**6**]} × 100%. Overlaid ^{1}H NMR spectra of the NH proton of (*S*)-G**6** [(○) red] and (*R*)-G**6** [(●) red] in the presence of an equal amount of TAMCSA **1a** in $CDCl_3$. [G**6**] = 5 mM. (Scans: 8; Data processing: MestReNova software; type of NMR probe: broadband gradient autotune).

■ ASSOCIATED CONTENT

Supporting Information

The Supporting Information is available free of charge at https://pubs.acs.org/doi/10.1021/acs.analchem.3c05395.

Synthetic procedures and structural characterization; NMR and HRMS spectra; and relative chiral recognition and DFT data (PDF)

■ AUTHOR INFORMATION

Corresponding Authors

Lin Ai − *College of Chemistry, Beijing Normal University, Beijing 100875, P. R. China;* orcid.org/0000-0001-9721-1493; Email: linai@bnu.edu.cn

Jiaxin Zhang − *College of Chemistry, Beijing Normal University, Beijing 100875, P. R. China;* Email: zhangjiaxin@bnu.edu.cn

Authors

Yu Wang − *College of Chemistry, Beijing Normal University, Beijing 100875, P. R. China*

Hongmei Zhao − *State Key Laboratory of Information Photonics and Communications, School of Science, Beijing University of Posts and Telecommunications, Beijing 100876, P. R. China;* orcid.org/0000-0002-6586-0357

Chunxia Yang − *College of Chemistry, Beijing Normal University, Beijing 100875, P. R. China*

Lixia Fang − *College of Chemistry, Beijing Normal University, Beijing 100875, P. R. China*

Li Zheng − *College of Chemistry, Beijing Normal University, Beijing 100875, P. R. China*

Hehua Lv − *College of Chemistry, Beijing Normal University, Beijing 100875, P. R. China*

https://doi.org/10.1021/acs.analchem.3c05395
Anal. Chem. 2024, 96, 5188−5194

Pericles Stavropoulos − *Department of Chemistry, Missouri University of Science and Technology, Rolla, Missouri 65409, United States;* orcid.org/0000-0003-0985-6203

Complete contact information is available at: https://pubs.acs.org/10.1021/acs.analchem.3c05395

Notes

The authors declare no competing financial interest.

■ ACKNOWLEDGMENTS

This work was supported by the Scientific Research Fund Performance Award of Beijing Normal University (award number 10200/111203277). Work in the Missouri Lab (P.S.) was supported by the National Institute of General Medical Science of the National Institutes of Health under award number R15GM117508 and R15GM139071.

■ REFERENCES

(1) Parker, D. *Chem. Rev.* **1991**, *91*, 1441−1457.
(2) Seco, J. M.; Quiñoá, E.; Riguera, R. *Chem. Rev.* **2004**, *104*, 17−117.
(3) Yang, L.; Wenzel, T.; Williamson, R. T.; Christensen, M.; Schafer, W.; Welch, C. J. *ACS Cent. Sci.* **2016**, *2*, 332−340.
(4) Kriegelstein, M.; Profous, D.; Přibylka, A.; Cankař, P. *J. Org. Chem.* **2020**, *85*, 12912−12921.
(5) Recchimurzo, A.; Balzano, F.; Uccello Barretta, G.; Gherardi, L. *J. Org. Chem.* **2022**, *87*, 11968−11978.
(6) Xiao, G. Y.; Xu, S.; Xie, C. C.; Zi, G. F.; Ye, W. P.; Zhou, Z. T.; Hou, G. H.; Zhang, Z. B. *Org. Lett.* **2021**, *23*, 5734−5738.
(7) Pan, J.-B.; Zhang, X.-G.; Shi, Y.-F.; Han, A.-C.; Chen, Y.-J.; Ouyang, J.; Li, M.-L.; Zhou, Q.-L. *Angew. Chem., Int. Ed.* **2023**, *62*, No. e202300691.
(8) Zou, Y. P.; Lai, Z. L.; Zhang, M. W.; Peng, J. Z.; Ning, S.; Li, C. C. *J. Am. Chem. Soc.* **2023**, *145*, 10998−11004.
(9) Qin, F.; Wang, C. Y.; Kim, D.; Wang, H.-S.; Zhu, Y.-K.; Lee, S. K.; Yao, G.-Y.; Liang, D. *J. Org. Chem.* **2021**, *86*, 1462−1470.
(10) Chen, M.; Guo, H.-M.; Di, S.-S.; Zhao, Y.; Zhou, D.-D.; Cao, Y.-W.; Tian, P.; Yang, Z.-H.; Zhao, H.-Y. *Chirality* **2023**, *35*, 376−386.
(11) Huang, B. L.; Xu, L. H.; Ying, J. X.; Zhao, Y. F.; Huang, S. H. *Anal. Chim. Acta* **2022**, *1230*, 340402.
(12) Dreisewerd, L.; Aspers, R. L. E. G.; Feiters, M. C.; Rutjes, F. P. J. T.; Tessari, M. *J. Am. Chem. Soc.* **2023**, *145*, 1518−1523.
(13) Zhang, H. Y.; Li, S.; Qu, A. H.; Hao, C. L.; Sun, M. Z.; Xu, L. G.; Xu, C. L.; Kuang, H. *Chem. Sci.* **2020**, *11*, 12937−12954.
(14) Meng, Y. Q.; Fan, J. B.; Wang, M. H.; Gong, W. B.; Zhang, J. P.; Ma, J. P.; Mi, H. Y.; Huang, Y.; Yang, S.; Ruoff, R. S.; Geng, J. X. *Angew. Chem., Int. Ed.* **2022**, *61*, No. e202117815.
(15) Teng, Y.; Gu, C. L.; Chen, Z. H.; Jiang, H.; Xiong, Y.; Liu, D.; Xiao, D. L. *Chirality* **2022**, *34*, 1094−1119.
(16) Rossino, G.; Robescu, M. S.; Licastro, E.; Tedesco, C.; Martello, I.; Maffei, L.; Vincenti, G.; Bavaro, T.; Collina, S. *Chirality* **2022**, *34*, 1403−1418.
(17) Collina, S.; Lucarini, S.; Benet-Buchholz, J.; Trapp, O.; Pescitelli, G.; Berova, N.; Berova, N. *Chirality* **2022**, *34*, 1491−1493.
(18) Lesot, P.; Aroulanda, C.; Berdagué, P.; Meddour, A.; Merlet, D.; Farjon, J.; Giraud, N.; Lafon, O. *Prog. Nucl. Magn. Reson. Spectrosc.* **2020**, *116*, 85−154.
(19) Aroulanda, C.; Lesot, P. *Chirality* **2022**, *34*, 182−244.
(20) Bian, G. L.; Yang, S. W.; Huang, H. Y.; Zong, H.; Song, L.; Fan, H. J.; Sun, X. Q. *Chem. Sci.* **2016**, *7*, 932−938.
(21) Recchimurzo, A.; Micheletti, C.; Uccello-Barretta, G.; Balzano, F. *J. Org. Chem.* **2021**, *86*, 7381−7389.
(22) Liu, L. Z.; Ma, C. G.; He, Q.; Huang, Y.; Duan, W. G. *Org. Chem. Front.* **2021**, *8*, 4144−4152.
(23) Groleau, R. R.; Chapman, R. S. L.; Lowe, J. P.; Lyall, C. L.; Kociok-Köhn, G.; James, T. D.; Bull, S. D. *Anal. Chem.* **2023**, *95*, 16801−16809.
(24) Lakshmipriya, A.; Chaudhari, S. R.; Suryaprakash, N. *Chem. Commun.* **2015**, *51*, 13492−13495.
(25) Li, G.-W.; Wang, X.-J.; Cui, D.-D.; Zhang, Y.-F.; Xu, R.-Y.; Shi, S.-H.; Liu, L.-T.; Wang, M.-C.; Liu, H.-M.; Lei, X.-X. *RSC Adv.* **2020**, *10*, 34605−34611.
(26) Tanaka, K.; Iwashita, T.; Sasaki, C.; Takahashi, H. *Tetrahedron: Asymmetry* **2014**, *25*, 602−609.
(27) Jung, S. H.; Kim, K. Y.; Ahn, A.; Lee, S. S.; Choi, M. Y.; Jaworski, J.; Jung, J. H. *New J. Chem.* **2016**, *40*, 7917−7922.
(28) Jain, N.; Khanvilkar, A. N.; Sahoo, S.; Bedekar, A. V. *Tetrahedron* **2018**, *74*, 68−76.
(29) Raval, H. B.; Bedekar, A. V. *ChemistrySelect* **2020**, *5*, 6927−6932.
(30) Nakatsuji, Y.; Nakahara, Y.; Muramatsu, A.; Kida, T.; Akashi, M. *Tetrahedron Lett.* **2005**, *46*, 4331−4335.
(31) Howard, J. A.; Nonn, M.; Fulop, F.; Wenzel, T. *Chirality* **2013**, *25*, 48−53.
(32) Zheng, Y.-S.; Zhang, C. *Org. Lett.* **2004**, *6*, 1189−1192.
(33) Seo, M.-S.; Kim, H. *J. Am. Chem. Soc.* **2015**, *137*, 14190−14195.
(34) Lv, C. X.; Feng, L.; Zhao, H. M.; Wang, G.; Stavropoulos, P.; Ai, L. *Org. Biomol. Chem.* **2017**, *15*, 1642−1650.
(35) Fang, L. X.; Lv, C. X.; Wang, G.; Feng, L.; Stavropoulos, P.; Gao, G. P.; Ai, L.; Zhang, J. X. *Org. Chem. Front.* **2016**, *3*, 1716−1724.
(36) Feng, L.; Gao, G. P.; Zhao, H. M.; Zheng, L.; Wang, Y.; Stavropoulos, P.; Ai, L.; Zhang, J. X. *J. Org. Chem.* **2018**, *83*, 13874−13887.
(37) Li, Y. L.; Zhao, H. M.; Ren, Y. Q.; Qiu, M.; Zhang, H. T.; Gao, G. P.; Zheng, L.; Stavropoulos, P.; Ai, L. *ChemistrySelect* **2023**, *8*, No. e202204039.
(38) Sun, Z. F.; Chen, Z. X.; Wang, Y. Q.; Zhang, X. B.; Xu, J.; Bian, G. L.; Song, L. *Org. Lett.* **2020**, *22*, 589−593.
(39) Jang, S.; Park, H.; Duong, Q. H.; Kwahk, E.-J.; Kim, H. *Anal. Chem.* **2022**, *94*, 1441−1446.
(40) Seo, M.-S.; Jang, S.; Kim, H. *Chem. Commun.* **2018**, *54*, 6804−6807.
(41) Zhang, X. B.; Xu, J.; Sun, Z. F.; Bian, G. L.; Song, L. *RSC Adv.* **2022**, *12*, 4692−4696.
(42) Yang, K.; Li, S.-Z.; Wang, Y.-H.; Zhang, W.-Z.; Xu, Z.-H.; Zhou, X.-Y.; Zhu, R.-X.; Luo, J.; Wan, Q. *RSC Adv.* **2014**, *4*, 6517−6526.
(43) Bai, L. W.; Chen, P.; Xiang, J. X.; Sun, J. R.; Lei, X. X. *Org. Biomol. Chem.* **2019**, *17*, 1466−1470.
(44) Malinowska, M.; Jarzyński, S.; Pieczonka, A.; Rachwalski, M.; Leśniak, S.; Zawisza, A. *J. Org. Chem.* **2020**, *85*, 11794−11801.
(45) Chen, Z. X.; Fan, H. J.; Yang, S. W.; Bian, G. L.; Song, L. *Org. Biomol. Chem.* **2018**, *16*, 8311−8317.
(46) Couffin, A.; Thillaye du Boullay, O.; Vedrenne, M.; Navarro, C.; Martin-Vaca, B.; Bourissou, D. *Chem. Commun.* **2014**, *50*, 5997−6000.
(47) Yang, S.-J.; Lee, J.-M.; Lee, G.-H.; Kim, N. Y.; Kim, Y.-S.; Gong, Y.-D. *Bull. Korean Chem. Soc.* **2014**, *35*, 3609−3617.
(48) Mizar, P.; Burrelli, A.; Günther, E.; Söftje, M.; Farooq, U.; Wirth, T. *Chem. Eur J.* **2014**, *20*, 13113−13116.
(49) Curini, M.; Epifano, F.; Maltese, F.; Marcotullio, M. C. *Tetrahedron Lett.* **2002**, *43*, 3821−3823.
(50) Kise, N.; Oike, H.; Okazaki, E.; Yoshimoto, M.; Shono, T. *J. Org. Chem.* **1995**, *60*, 3980−3992.
(51) Kise, N.; Iwasaki, T.; Yasuda, Y.; Sakurai, T. *Tetrahedron Lett.* **2008**, *49*, 7074−7077.
(52) Nair, V.; Khatik, G.; Khurana, R.; Kumar, V. *Synthesis* **2011**, *2011*, 3123−3132.
(53) Ulatowski, F.; Dabrowa, K.; Balakier, T.; Jurczak, J. *J. Org. Chem.* **2016**, *81*, 1746−1756.
(54) Becke, A. D. *J. Chem. Phys.* **1993**, *98*, 5648−5652.